EDUCATUM JSMT Vol. 12 SPECIAL ISSUE (2025)
ISSN 2289-7070 / e-ISSN 2462-2451(77-89)
https://ejournal.upsi.edu.my/index.php/EJSMT/index

A Comprehensive Study of 4-Sulfocalix[4]arene Thin Films with Atomic Force Microscopy: Thickness and Topographical Analysis

Farish Armani Hamidon[1], Faridah Lisa Supian[1*], Mazlina Mat Darus[1], Nur Farah Nadia Abd Karim[1], Wong Yeong Yi[1]

[1]Department of Physics, Faculty of Science and Mathematics, Universiti Pendidikan Sultan Idris, 35900, Tanjong Malim, Perak, Malaysia

*Corresponding author: faridah.lisa@fsmt.upsi.edu.my

Received: 1 Jan 2025; **Revision:** 20 February 2025; **Accepted:** 25 March 2025; **Published:** 28 April 2025

To cite this article (APA): Hamidon, F. A., Supian, F. L., Mat Darus, M.., Abd Karim, N. F. N., & Wong, Y. Y. (2025). A Comprehensive Study of 4-Sulfocalix[4]arene Thin Films with Atomic Force Microscopy: Thickness and Topographical Analysis. EDUCATUM Journal of Science, Mathematics and Technology, 12, 77-89. https://doi.org/10.37134/ejsmt.vol12.sp.8.2025

To link to this article: https://doi.org/10.37134/ejsmt.vol12.sp.8.2025

ABSTRACT

This study aims to characterise 4-Sulfocalix[4]arene (SC[4]) thin films using Atomic Force Microscopy (AFM) in analysing its thickness and surface morphology. Quartz substrates were cleaned using ultrasonic cleaning with an Elmasonic P70H. SC[4] thin films were then fabricated on a quartz surface using WS-400BZ-6NPP/A1/AR1 model spin coater from Laurel Technologies, producing thin films with 5, 10, 15, and 20 layers. Each thin film was characterised in the tapping mode of the AFM Park System NX-10. Scans were conducted on different film areas of different scales, and the data were analysed using XEI Data Processing and Analysis Software. Height measurements obtained via Line Profile analysis revealed a progressive increase in film thickness with the additional layers, demonstrating a significant linear relationship. AFM images showed precise 2D and 3D surface topography, indicating that the thin films became uneven and non-uniform with the addition of more layers. The findings demonstrated a linear relationship between film thickness and the number of layers, measuring 58.175 nm for 5 layers, 77.626 nm for 10 layers, 84.608 nm for 15 layers, and 94.806 nm for 20 layers. The surface roughness of thin films was also determined, and it is significantly influenced by the number of layers, as illustrated by the root mean square roughness (R_q). The values were found to be 26.512 for 5 layers, 29.777 for 10 layers, 30.177 for 15 layers, and 31.093 for 20 layers, respectively. This increase in surface irregularity indicates that the deposition process leads to progressively irregular surfaces with an additional number of layers, as proven by equivalent studies on thin films. This study emphasised the effectiveness of AFM in thin film research by demonstrating its precision in measuring thickness and analysing surface topography.

Keywords: 4-Sulfocalix[4]arene, Atomic Force Microscope, Spin-Coating Method, Thickness Measurement, Topographical Analysis

INTRODUCTION

Calixarenes are organic macrocyclic oligomers synthesised by the base-catalysed condensation of formaldehyde and para-alkyl phenol [1], [2]. These phenolic methylene-bridged macrocycles are composed of alkylidene groups that connect repeating phenol units at positions two and six, and its basket-like structure enables the alteration of the upper and lower rims [3], [4], [5]. Modifying and adjusting the lower and upper rims by incorporating specific functional groups or molecules can improve the selectivity of calixarenes for various target guest molecules.

Scientists have conducted extensive studies over the past three decades to synthesise and investigate numerous types of derivatives and chemical modifications of calixarenes to attain specific properties that are appropriate for a wide range of applications [6], [7], [8]. These applications include detecting contaminants, metal ions, and biomolecules through chemical sensing and its acknowledged function in catalysing organic synthesis [9], [10], [11], [12], [13], [14], [15]. Additionally, the electrochemical properties of calixarenes have stimulated investigation into its potential for environmental remediation by capturing toxic substances and for the development of electrochemical sensors and devices [16], [17], [18]. Calixarene derivatives are desirable precursor materials in synthetic organic chemistry due to the widely accessible polyfunctional hydroxyl groups, which can be quickly incorporated into other functional groups [19], [20]. One of the derivatives of the calixarene family, 4-Sulfocalix[4]arene (SC[4]), contains the sulfonate groups in its upper rim and aromatic rings [21], [22], [23], as seen in **Figure 1**. SC[4]'s phenolic hydroxyl groups produce intramolecular solid hydrogen bonding, and it also contains acidic sulfonate and acidic phenolic groups.

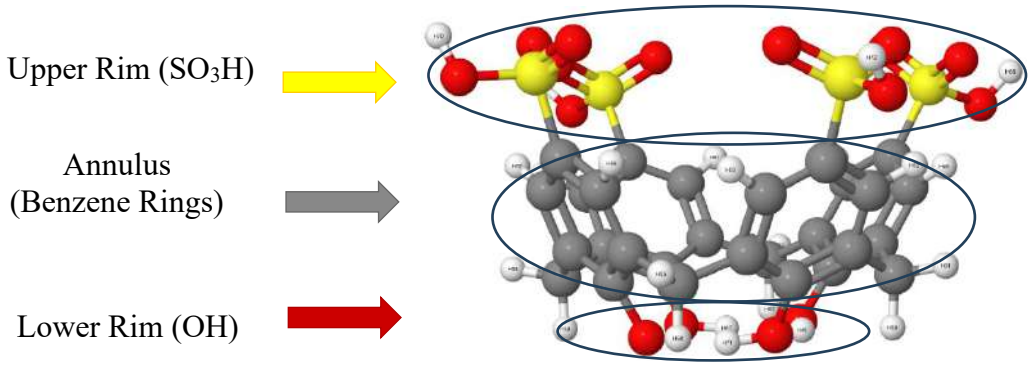

Figure 1: Three-dimensional representation of 4-Sulfocalix[4]arene with labels in the upper and lower rims, with atoms coloured according to the CPK model: black for carbon, red for oxygen, yellow for sulfur and white for hydrogen

Various fabrication techniques are available for depositing calixarenes and its derivatives, such as thin films with desired properties and application fields. One such thing is the spin coating method, which uses centrifugal force to distribute its solution on a substrate surface to form thin layers on flat surfaces evenly. Another method is Langmuir-Blodgett (LB), which allows for the precise deposition of monolayers on different surfaces. The films can be modified to adjust its thickness and functional properties, enabling its use in detecting environmental pollutants or enhancing catalytic reactions. Lastly is the technique called drop casting, where a solution containing calixarenes is deposited onto a substrate in the form of droplets, allowing for the formation of thin films upon solvent evaporation when in contact with a hot surface [24], [25].

The two primary objectives in thin-film coating fabrications are surface protection and surface functionalisation [26]. Atomic Force Microscopy (AFM) is a sophisticated and highly effective scanning probe technique renowned for achieving resolutions on a scale of fractions of an Angstrom, surpassing conventional optical microscopes by over a thousand times. This technique is instrumental in the study of thin film surface topography [27], [28]. AFM employs a cantilever made from silicon or silicon nitride at the micro and nanoscales. This cantilever features a sharpened tip used to conduct nanoscale scans on the sample surface. By measuring the interaction forces between the tip and the surface, AFM can determine various types of forces, including mechanical contact force, magnetic, van der Waals interactions, electrostatic, capillary, chemical, and steric force, depending on the experimental objectives and characterisations.

Furthermore, AFM involves scanning a sample's surface with a pointed tip attached to the end of a microcantilever in order to measure surface forces on thin coatings. It operates in three modes: contact, non-contact, and tapping. Specifically, in non-contact mode, the cantilever point remains 5-15 nm above the surface, while in contact mode, it remains in close proximity. However, contact mode encounters difficulties such as potential malfunction, damage during the scanning process and increased tip wear. The tapping mode addressed these problems by reducing electrostatic forces and adhesion through its intermittent contact mechanism, managing tip interaction with rough surfaces, and minimising friction.

Additionally, AFM provides numerical data on surface and structural properties, including surface morphology of thin films [29], [30], [31], grain distribution [32] and power spectral density (PSD) functions [33]. Notably, the sample does not need to be conductive and can be applied to either conductive or non-conductive materials without the requirements for additional treatment. This is advantageous when electrical current measurements are unnecessary, as AFM senses mechanical deflection rather than relying on electrical properties [34], [35], [36], [37].

Consequently, this method can directly correlate mechanical interactions with surface profiles and film thickness [34], [35]. For high resolution, the cantilever tip must be extremely delicate, with the finest tips measuring only a few nanometers. Moreover, AFM can analyse surface properties and geometry without requiring the sample to be optically reflective or conductive. It generates three-dimensional surface profiles and captures deflections using raster scanning. To be more precise, the tip is positioned in a transition region, such as a border or furrow, to measure the vertical distance differences between the film's surface and the underlying substrate, thereby providing precise measurements of thin film thickness [35].

Surface topography encompasses the various three-dimensional characteristics of a surface, such as micro and nano-pores, nanotubes, gratings, columns, pits, and scattered grooves, that collectively shape its roughness. This roughness, influenced by environmental factors, surface chemistry, and material properties, defines the surface's texture. It incorporates attributes such as roughness, waviness, grain, and defects, which are deviations from an ideal flat or spherical surface. These features are essential for elucidating surface-related phenomena, including wetting, adhesion, adsorption, and friction, as well as optimising surface functionalities and comprehending material interactions in industrial and scientific applications [38], [39], [40], [41], [42].

The three-dimensional topology of a surface is defined by its measurable deviations, which include both consistent and sporadic height variations and irregularities. These variations determine the surface's degree of smoothness or roughness. It is typically quantified using parameters such as mean roughness (R_a) and root mean square roughness (R_q), which represent the average height deviations of microscopic peaks and valleys distributed across the surface of the films. This characteristic is essential for comprehending both the functional and structural properties of material surfaces, as it provides critical observations into their microcosmic geometric and shape properties [43], [44], [45], [46], [47], [48].

This paper aims to describe and determine the thickness and topographical analysis of SC[4] thin films using an atomic force microscope for the boundless applications that will become possible in the following decades, such as nano adsorbents and other fields progressing towards nanoscales. The novelty of this work lies in the characterisation of SC[4] films, among calixarene derivatives that have rarely been described in terms of film features due to their distinct properties from the parent calixarene. The parent calixarene is frequently fabricated using a common and standard method for calixarene, the Langmuir

method. Additionally, it is unique in that it is characterised using AFM to elucidate its thin film properties, a characterisation that has never been undertaken before also for thin films of SC[4].

MATERIALS AND METHODS

Solution preparation

The SC[4] solution was prepared by measuring 2.5 mg of SC[4] grains on an electronic digital balance and transferring them to a sterile vial. The SC[4] was diluted in 10 ml of Deionised water (DI water) and stirred or swirled to ensure homogenous dissolving. The solution had been prepared for further use and had a concentration of 0.25 mg ml^{-1} [49], [50].

Fabrication of thin film using the spin coating method

The Elmasonic P70H Ultrasonic cleansing instrument was utilised to prepare the clean substrate prior to the fabrication of films. Acetone, propanol, and DI water were employed to clean the surface of a 25 mm by 25 mm quartz substrate in order to eliminate any residue or impurities. The substrate was subsequently immersed in 1,1,1,3,3,3-hexamethyldisilazane, $C_6H_{19}NSi_2$ (HMDS) vapour for a period of one day or more, stored in a Petri dish and sealed with a parafilm to prevent the leakage of HDMS vapour [51].

The SC[4] thin film was fabricated using the spin coating technique, which employs centrifugal force to distribute thin layers on flat surfaces evenly. A single thin film layer was formed by depositing the SC[4] solution onto a glass quartz substrate and rotating it at 2000 rpm for 15 seconds. In order to obtain the required number of layers (5, 10, 15, and 20), this procedure was repeated. Concurrent with the spin coating procedure, the substrate was dry with a nitrogen gun [52], [53], [54], [55], [56], [57].

Characterisation of the calixarene thin films with AFM

AFM is a standard scanning microscope utilised to obtain a three-dimensional and high-resolution image of the sample surface. In this study, the AFM Park System NX-10 model at the i-CRIM lab, National University of Malaysia, depicted in **Figure 2(a)**, was employed to characterise the SC[4] films for both thicknesses and morphological analysis and the result was analysed with XEI Data Processing and Analysis Software (XEI) by the Park System. **Figure 2(b)** shows a schematic diagram of the measurement and a brief view of its components used for thin film measurements and surface characterisation**.** The characterisation was performed beneath atmospheric pressure and circumstances in tapping mode. The measurement used the scanning frequencies of 0.8 Hz was applied to scanning areas of 10 µm x 10 µm, 30 µm x 30 µm and 5 µm x 5 µm, respectively, for each film layer.

Before performing the analysis, the films underwent a gentle cleaning process with a cotton swab in a designated small area of the substrate surface, and the back of each substrate was marked with a non-permanent marker. This step aimed to distinguish between the regions with and without SC[4] coating. The film was then put onto an AFM sample stage. The next step involves thoroughly cleaning and carefully installing a cantilever with an adequate tip for the analysis. The AFM controls software was then launched on a computer, and a connection with the AFM was established. The sample stage was gradually brought into proximity with the cantilever, ensuring a slow approach to the sample surface to avoid any sudden contact that could cause damage to it. The ambient temperature of 22 ºC and relative humidity of 47 % remained unchanged throughout the image acquisition process in these AFM analyses.

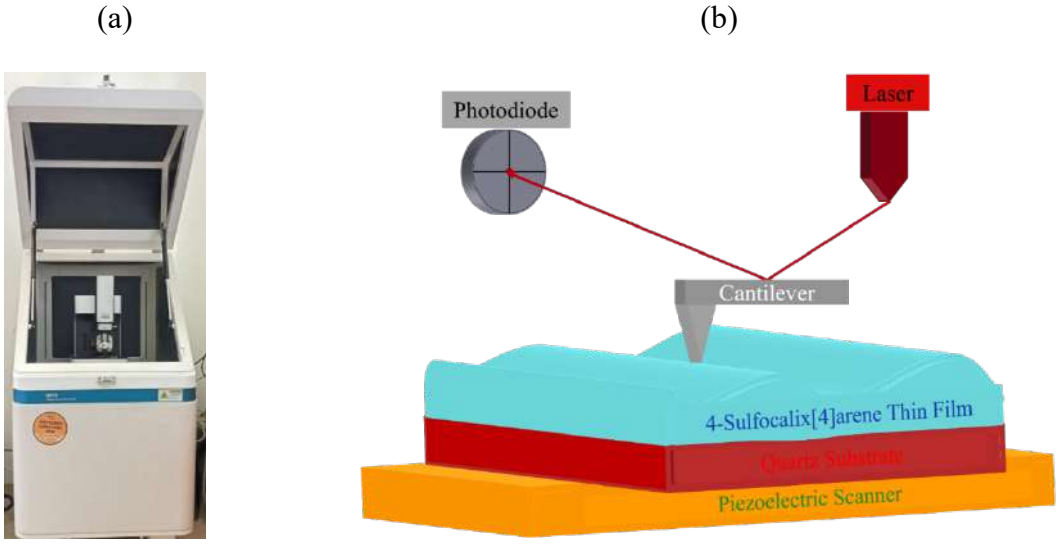

Figure 2. (a) The Atomic Force Microscope (AFM Park System NX-10 Model) used in this study (b) Schematic diagram of AFM during the scanning process on the SC[4] Films.

The height measurements for each SC[4] thin film difference in a number of layers were conducted using the Line Profile analysis functions in the XEI software. First, a horizontal line profile was inserted into the image and positioned at the desired points across the surface of the films. The line was ensured to cross representative areas of the film's features of interest, touching both the film areas (brighter cyan or white) and the substrate (darker colour or black). Once the line profile is placed, the software will generate a height profile along the selected line, displaying height variations across the surface. Subsequently, a cursor pair was inserted on the line profile to measure the height difference, signifying thickness (ΔY) and distance (ΔX) between two data points. One cursor was positioned on the lowest non-coating region or substrate surface, while the other was placed on the highest point of the films within the same line profile. However, the cursor was deliberately not positioned at the absolute maximum peak of the line profile, particularly in the whitest region denoting the highest altitude or steepest peak. This precaution was taken to avoid potential errors resulting from non-uniform readings.

Eventually, the surface roughness analysis of SC[4] thin films, varying in the number of layers, was carried out using the roughness tab in the XEI software. The measurement for R_q was taken by choosing a constant region of interest measuring 2.5 µm by 2.5 µm. This region was maintained across all films to ensure uniformity in the measurements despite variations in film coverage areas. The roughness parameter, including Root Mean Square (R_q) roughness, was computed and generated automatically upon selecting the designated region in the processed images. Subsequently, the roughness profiles for the selected regions were recorded in a table with its respective number of film layers.

RESULTS AND DISCUSSIONS

Thicknesses measurements and topographical analysis of SC[4] thin films using atomic force microscopes

Figure 3 displays an AFM image of SC[4] thin films with varying numbers of layers (5, 10, 15, and 20) fabricated on the quartz substrate. The scanned areas differ and are shown in varying shades, with brighter colours (ranging from white to dark cyan), signifying higher altitudes. AFM imaging details the surface topography of thin films, and the varying shades in the image suggest variations in surface height. Approximately half of the scanned region appears in dark cyan or black, showing the exposed surface of

the substrate. The analysis employed both 2-dimensional (2D) and 3-dimensional (3D) views to capture comprehensive line profiles [58], [59].

The line profile analysis performed on the AFM images indicates a progressive increase in the thickness of the film with the deposition of the additional layers, which strongly supports this interaction from the AFM data. **Figure 4** further illustrates the AFM images of SC[4] thin films, showcasing its surface morphologies in both 2D and 3D perspectives. The image profiles reveal that films formed at varying numbers of layers exhibit uneven and non-uniform surfaces. This unevenness can be attributed to the spin coating fabrication method, wherein the solution is dispersed outward due to centrifugal force, leading to random distribution and variation in thickness as the number of layers increases.

Additionally, the molecular orientation of SC[4] in the films will be distributed arbitrarily, with some molecules orientated vertically upwards and others downwards. However, the sulfonate groups (SO_3H) of SC[4] will be predominantly oriented upwards relative to the substrate surface. This upward orientation of SC[4], with sulfonate groups facing upwards, enhances the films' ability to interact with various molecules through different chemical interactions, including electrostatic and molecular bonding. Therefore, the presence of sulfonate groups oriented upward can improve and achieve the desired binding properties and functionalities of thin films with specific characteristics and specifications in various applications. For instance, this can enhance the adhesion of guest molecules and the catalytic activities of the SC[4] thin films [60], [61], [62].

Besides, several factors contribute to the non-uniformity of films in the spin coating process, such as air circulation disturbances that generate irregular shear forces, complex interactions between centrifugal and shear forces on non-circular substrates, and fluctuations in solvent evaporation rates. Edge effects on substrates, mainly rectangular shapes, also affect defects and uneven thickness. In addition to the substrate geometry and curvature, these parameters make it difficult to achieve a consistent layer of uniform film thickness [63], [64]. Surface irregularities in adsorption processes generate localised high-energy areas that increase binding affinities for particular molecules. These roughness and irregularities, also known as surface defects or heterogeneities, are pivotal in adsorption as they offer active sites with elevated binding energies relative to more uniform surfaces. The distribution of adsorption site energies in porous materials highlights the significance of high-energy sites in influencing the efficiency and selectivity of adsorption processes [65], [66], [67].

The thickness measurement of the SC[4] thin films, generated by the line profile analysis of the images, is then plotted in the graph shown in **Figure 4** (Left). Finally, **Table 1** provides a detailed line profile analysis, correlating the number of layers with the respective horizontal and vertical distances and the angle between marked cursors on the line profile. In this table, N denotes the number of layers, ΔX and ΔY represent the horizontal and vertical distance, respectively, between two points marked with a cursor pair on the line profile, and the angle (°) refers to the angle between these two distances, ΔX and ΔY. The ΔY is equivalent to the thickness of thin films in this study. The results demonstrate a linear relationship between the number of layers and the film height, suggesting a uniform deposition process.

Furthermore, it was shown that increasing the number of layers of thin films affected its surface roughness, quantified through its root mean square roughness, R_q. Precisely, the R_q values were 26.512 nm for 5 layers, 29.777 nm for 10 layers, 30.177 nm for 15 layers, and 31.093 nm for 20 layers, as plotted in corresponding **Figure 4** (Right) and **Table 2**. This progressive increase in surface roughness with additional layers indicates the irregular deposition process commonly assosiated with spin-coated thin films. [68], [69],

[70]. The surface morphology of spin-coated thin films often demonstrates increased roughness with more layers, resembling granular and clustered properties. This roughness arises from the aggregation of surface irregularities, incosistent growth layers across cycles, and insufficient smoothing during deposition and drying process. Solvent effects, crystallisation, island formation, and suboptimal layer adhesion significantly exacerbate these surface characteristics. Additionally, the rapid evaporation of solvents intensifies these effects, causing a more uneven and textured surface as the number of layers increases [71], [72]. These outcomes corresponded with the results of analogous studies, which indicated that the incorporation of layers typically leads to enhanced surface irregularities in thin films

In summary, it can be concluded that the thickness and surface texture of the film are both affected by the addition of additional layers to the thin film coating. The surface roughness and thickness increase in direct proportion to the number of thin film layers. Thin films with a rough surface offer numerous advantages, including increased mechanical stability, an enhancement to interaction behaviour, a larger surface area and improved coating adhesion [73], [74], [75], [76]. This is notably advantageous in applications such as sensor technology and catalysis, as it enables more extensive interaction with the molecules in the surrounding area. Furthermore, molecular interactions, including crystallisation and dissolution dynamics in vapour-deposited films, can be influenced by uneven surfaces. Mechanical stability is also essential for preserving integrity during interactions with other materials and under pressure. Nevertheless, uneven surfaces have the potential to impede uniformity, which could result in inconsistent performance in specific applications. It is crucial for optimising functionality by combining roughness with other surface properties.

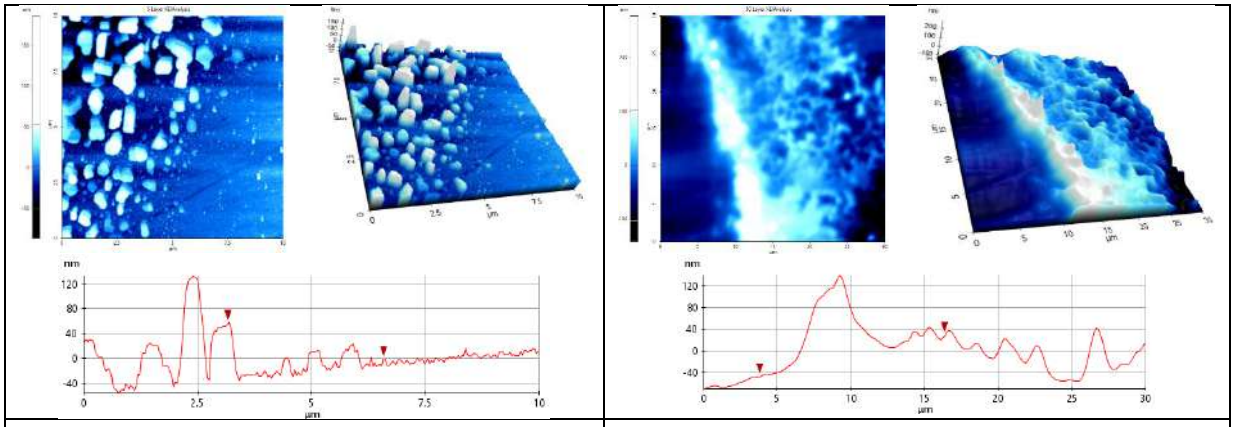

(a) 5 Layers

(b) 10 Layers

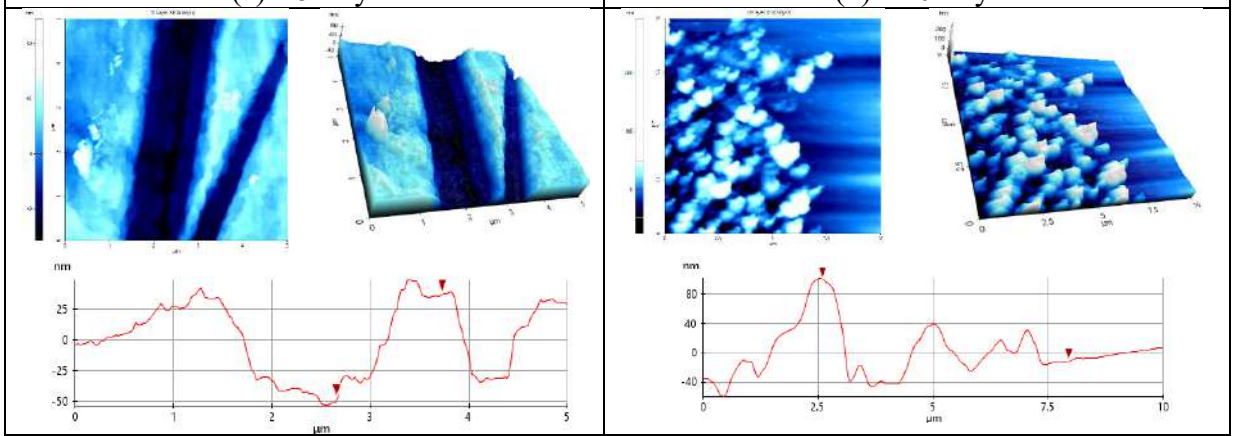

(c) 15 Layers

(d) 20 Layers

Figure 3. AFM images of SC[4] films with varying numbers of layers: (a) 5 Layers, (b) 10 Layers, (c) 15 Layers, and (d) 20 Layers, presented in both 2-dimensional (left) and 3-dimensional (right) views with its corresponding line profiles.

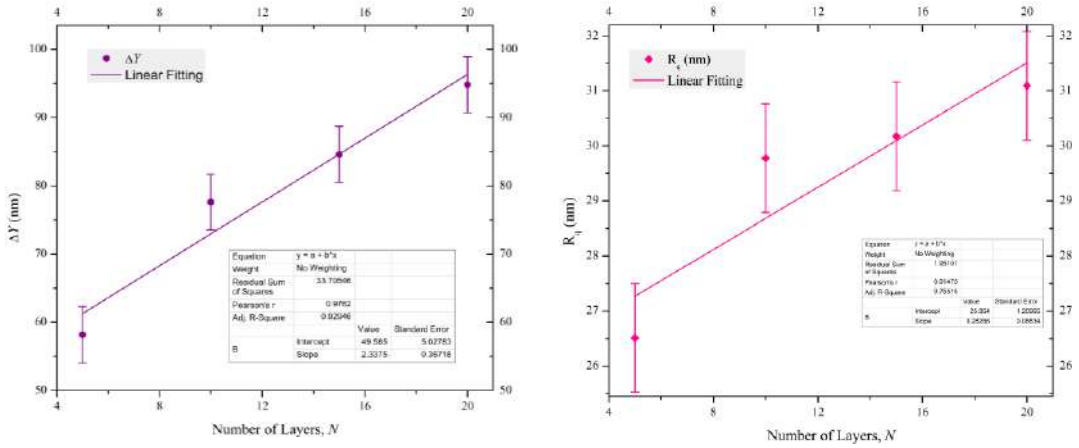

Figure 4. The Thickness, ΔY (Left) and Surface Roughness, R_q (Right) of SC[4] Thin Films as a Function of the Number of Layers

Table 1. Line profile analysis of multilayer SC[4] thin films determined from AFM images

Number of Layers, N	ΔX (μm)	ΔY (nm)	Angle (°)
5	3.418	58.175	0.975
10	12.539	77.626	0.355
15	0.996	84.608	4.855
20	2.695	94.806	-2.015

Table 2. Roughness analysis of multilayer SC[4] thin films determined from AFM images

Number of Layers, N	R_q (nm)
5	26.512
10	29.777
15	30.177
20	31.093

CONCLUSION

The primary objectives of this study are to characterise and analyse both the thickness, ΔY and surface roughness, R_q of 4-Sulfocalix[4]arene (SC[4]) thin films using an atomic force microscope. SC[4] thin films with a different number of layers (5, 10, 15, 20) were successfully fabricated. AFM analysis was utilised to ascertain the topographical properties and thickness of these films by analysing surface profiles and measuring height deviations across line profiles.

The results obtained show that the surface profiles of the films are non-uniform and irregular across all layer configurations. In addition, the line profile analysis revealed that the thickness of the thin films increases in proportion to the number of layers, indicating a linear relationship between the number of layers and the thickness of the film.

In addition to thickness, the surface roughness of the films was also quantified using the root mean square roughness, R_q. The results show that the surface irregularity of the coatings increases as the number of layers increases. This observation further illustrates the influence of layer aggregation on film properties, which highlights a correlation between the irregularity of the film surface and the number of layers. Certain

advantages may be offered upon the desired properties and functionalities by the surface irregularities of the films for specific applications.

In closing, the insight gathered from this study offers significant advantages for applications and future research that involve SC[4] and other calixarene derivatives in thin film fabrication. Implementing these thin films in various nanotechnology fields, such as environmental science, optoelectronics, and materials science, can facilitate advancements and a deeper comprehension of these areas.

DECLARATION OF INTEREST

The authors declare that there is no conflict of interest.

ACKNOWLEDGEMENT

The authors would like to express gratitude to Sultan Idris Education University (UPSI), Malaysia, and acknowledge the i-CRIM lab for the analytical services provided.

REFERENCES

[1] L. Garcia-Rio, N. Basílio, and V. Francisco, 'Counterion effect on sulfonatocalix[n]arene recognition', *Pure Appl. Chem.*, vol. 92, no. 1, pp. 25–37, Jan. 2020, doi: 10.1515/pac-2019-0305.
[2] S. Shinkai, 'Calixarenes-The Third Generation of Supramolecules', *Tetrahedron*, vol. 49, no. 40, pp. 8933–8968, 1993.
[3] A. de Fatima, S. Fernandes, and A. Sabino, 'Calixarenes as New Platforms for Drug Design', *Curr. Drug Discov. Technol.*, vol. 6, no. 2, 2009, doi: 10.2174/157016309788488302.
[4] H. Li and Y. W. Yang, 'Gold nanoparticles functionalized with supramolecular macrocycles', *Chin. Chem. Lett.*, vol. 24, no. 7, pp. 545–552, 2013, doi: 10.1016/j.cclet.2013.04.014.
[5] V. Bohmer, 'Calixarenes, Macrocycles with (Almost) Unlimited Possibilities', *Angew. Chem. Int. Ed. Engl.*, vol. 34, no. 7, pp. 713–745, 1995.
[6] S. Moffa *et al.*, 'Synthesis, characterization, and computational study of aggregates from amphiphilic calix[6]arenes. Effect of encapsulation on degradation kinetics of curcumin', *J. Mol. Liq.*, vol. 368, p. 120731, Dec. 2022, doi: 10.1016/j.molliq.2022.120731.
[7] E. Español and M. Villamil, 'Calixarenes: Generalities and Their Role in Improving the Solubility, Biocompatibility, Stability, Bioavailability, Detection, and Transport of Biomolecules', *Biomolecules*, vol. 9, no. 3, p. 90, Mar. 2019, doi: 10.3390/biom9030090.
[8] R. Ludwig, 'Calixarenes in analytical and separation chemistry', *Fresenius J. Anal. Chem.*, vol. 367, no. 2, pp. 103–128, May 2000, doi: 10.1007/s002160051611.
[9] G. Sachdeva *et al.*, 'Calix[n]arenes and its derivatives as organocatalysts', *Coord. Chem. Rev.*, vol. 472, p. 214791, Dec. 2022, doi: 10.1016/j.ccr.2022.214791.
[10] C. Jin Mei and S. Ainliah Alang Ahmad, 'A review on the determination heavy metals ions using calixarene-based electrochemical sensors', *Arab. J. Chem.*, vol. 14, no. 9, Sep. 2021, doi: 10.1016/j.arabjc.2021.103303.
[11] A. Gorbunov *et al.*, 'Selective azide-alkyne cycloaddition reactions of azidoalkylated calixarenes', *Org. Chem. Front.*, vol. 7, no. 17, pp. 2432–2441, Sep. 2020, doi: 10.1039/d0qo00650e.
[12] A. Awasthi, P. Jadhao, and K. Kumari, 'Clay nano-adsorbent: structures, applications and mechanism for water treatment', *SN Appl. Sci.*, vol. 1, no. 9, Sep. 2019, doi: 10.1007/s42452-019-0858-9.

[13] R. Sivashankar, A. B. Sathya, K. Vasantharaj, and V. Sivasubramanian, 'Magnetic composite an environmental super adsorbent for dye sequestration - A review', *Environ. Nanotechnol. Monit. Manag.*, vol. 1–2, pp. 36–49, Nov. 2014, doi: 10.1016/j.enmm.2014.06.001.
[14] V. Montes-García, J. Pérez-Juste, I. Pastoriza-Santos, and L. M. Liz-Marzán, 'Metal nanoparticles and supramolecular macrocycles: A tale of synergy', *Chem. - Eur. J.*, vol. 20, no. 35, pp. 10874–10883, Aug. 2014, doi: 10.1002/chem.201403107.
[15] G. Mcmahon, S. O'malley, K. Nolan, and D. Diamond, 'Important calixarene derivatives-their synthesis and applications', *Arkivoc*, vol. 2003, no. 7, pp. 23–31, Apr. 2003, doi: http://dx.doi.org/10.3998/ark.5550190.0004.704.
[16] N. I. Ruslan, D. C. K. Lim, S. A. Alang Ahmad, S. F. N. Abdul Aziz, F. L. Supian, and N. A. Yusof, 'Ultrasensitive electrochemical detection of metal ions using dicarboethoxycalixarene-based sensor', *J. Electroanal. Chem.*, vol. 799, pp. 497–504, Aug. 2017, doi: 10.1016/j.jelechem.2017.06.038.
[17] A. Shah, 'A Novel Electrochemical Nanosensor for the Simultaneous Sensing of Two Toxic Food Dyes', *ACS Omega*, vol. 5, no. 11, pp. 6187–6193, Mar. 2020, doi: 10.1021/acsomega.0c00354.
[18] S. Abubakar, T. Skorjanc, D. Shetty, and A. Trabolsi, 'Porous Polycalix[n]arenes as Environmental Pollutant Removers', *ACS Appl. Mater. Interfaces*, vol. 13, no. 13, pp. 14802–14815, Apr. 2021, doi: 10.1021/acsami.0c23074.
[19] S. Pilato *et al.*, 'Calixarene-based artificial ionophores for chloride transport across natural liposomal bilayer: Synthesis, structure-function relationships, and computational study', *Biochim. Biophys. Acta BBA - Biomembr.*, vol. 1863, no. 10, p. 183667, Oct. 2021, doi: 10.1016/j.bbamem.2021.183667.
[20] T. Nishikubo, A. Kameyama, and H. Kudo, 'Novel High Performance Materials. Calixarene Derivatives Containing Protective Groups and Polymerizable Groups for Photolithography, and Calixarene Derivatives Containing Active Ester Groups for Thermal Curing of Epoxy Resins', *Polym. J.*, vol. 35, no. 3, pp. 213–229, 2003, doi: http://dx.doi.org/10.1295/polymj.35.213.
[21] X. Tian *et al.*, '4-Sulfocalix[4]arene/Cucurbit[7]uril-Based Supramolecular Assemblies through the Outer Surface Interactions of Cucurbit[n]uril', *ACS Omega*, vol. 3, no. 6, pp. 6665–6672, Jun. 2018, doi: 10.1021/acsomega.8b00829.
[22] X. Y. Hu, S. Peng, D. S. Guo, F. Ding, and Y. Liu, 'Molecular recognition of amphiphilic p - sulfonatocalix[4]arene with organic ammoniums', *Supramol. Chem.*, vol. 27, pp. 336–345, 2015, doi: 10.1080/10610278.2014.967242.
[23] S. Shinkai, S. Mori, T. Tsubaki, T. Sone, and O. Manabe, 'New water-soluble host molecules derived from calix[6]arene', *Tetrahedron Lett.*, vol. 25, no. 46, 1984, doi: 10.1016/S0040-4039(01)81592-6.
[24] P. Shivappa Adarakatti, C. W. Foster, C. E. Banks, A. K. N. S., and P. Malingappa, 'Calixarene bulk modified screen-printed electrodes (SPCCEs) as a one-shot disposable sensor for the simultaneous detection of lead(II), copper(II) and mercury(II) ions: Application to environmental samples', *Sens. Actuators Phys.*, vol. 267, pp. 517–525, Nov. 2017, doi: 10.1016/j.sna.2017.10.059.
[25] Ö. Mermer, S. Okur, F. Sümer, C. Özbek, S. Sayın, and M. Yılmaz, 'Gas Sensing Properties of Carbon Nanotubes Modified with Calixarene Molecules Measured by QCM Techniques', *Acta Phys. Pol. A*, vol. 121, no. 1, pp. 240–242, Jan. 2012, doi: 10.12693/APhysPolA.121.240.
[26] X. Liang, D. M. King, and A. W. Weimer, 'Ceramic ultra-thin coatings using atomic layer deposition', in *Ceramic Nanocomposites*, Rajat Banerjee and Indranil Manna, Eds., Elsevier, 2013, pp. 257–283. doi: 10.1533/9780857093493.2.257.
[27] R. Asmatulu and W. S. Khan, 'Characterization of electrospun nanofibers', in *Synthesis and Applications of Electrospun Nanofibers*, Elsevier, 2019, pp. 257–281. doi: 10.1016/B978-0-12-813914-1.00013-4.
[28] M. F. Erinosho and E. T. Akinlabi, 'Estimation of Surface Topography and Wear Loss of Laser Metal-Deposited Ti6Al4V and Cu', *Adv. Eng. Mater.*, vol. 18, no. 8, pp. 1396–1405, Aug. 2016, doi: 10.1002/adem.201600062.
[29] Z.-N. Fang, B. Yang, M.-G. Chen, C.-H. Zhang, J.-P. Xie, and G.-X. Ye, 'Growth and morphology of ultra-thin Al films on liquid substrates studied by atomic force microscopy', *Thin Solid Films*, vol. 517, no. 11, pp. 3408–3411, Apr. 2009, doi: 10.1016/j.tsf.2009.01.017.
[30] M. Kwoka, L. Ottaviano, and J. Szuber, 'AFM study of the surface morphology of L-CVD SnO2 thin films', *Thin Solid Films*, vol. 515, no. 23, pp. 8328–8331, Sep. 2007, doi: 10.1016/j.tsf.2007.03.035.

[31] J. Xie, X. Lu, Y. Zhu, C. Liu, N. Bao, and X. Feng, 'Atomic force microscopy (AFM) study on potassium hexatitanate whisker (K2O·6TiO2)', *J. Mater. Sci.*, vol. 38, no. 17, pp. 3641–3646, Sep. 2003, doi: 10.1023/A:1025685516330.
[32] M. Cremona *et al.*, 'Grain size distribution analysis in polycrystalline LiF thin films by mathematical morphology techniques on AFM images and X-ray diffraction data', *J. Microsc.*, vol. 197, no. 3, pp. 260–267, Mar. 2000, doi: 10.1046/j.1365-2818.2000.00661.x.
[33] Y. Gong, S. T. Misture, P. Gao, and N. P. Mellott, 'Surface Roughness Measurements Using Power Spectrum Density Analysis with Enhanced Spatial Correlation Length', *J. Phys. Chem. C*, vol. 120, no. 39, pp. 22358–22364, Oct. 2016, doi: 10.1021/acs.jpcc.6b06635.
[34] T. Ando, T. Uchihashi, and S. Scheuring, 'Filming biomolecular processes by high-speed atomic force microscopy', *Chem. Rev.*, vol. 114, no. 6, pp. 3120–3188, Mar. 2014, doi: 10.1021/cr4003837.
[35] G. Binnig, C. F. Quate' ', E. L. Gi, and C. Gerber, 'Atomic Force Microscope', *Phys. Rev. Lett.*, vol. 56, no. 9, pp. 930–933, Mar. 1996, doi: 10.1103/PhysRevLett.56.930.
[36] P. S. Liu and G. F. Chen, 'Characterization Methods', in *Porous Materials*, Elsevier, 2014, pp. 411–492. doi: 10.1016/B978-0-12-407788-1.00009-5.
[37] P. J. D. Whiteside, J. A. Chininis, and H. K. Hunt, 'Techniques and challenges for characterizing metal thin films with applications in photonics', *Coatings*, vol. 6, no. 3, pp. 1–26, Sep. 2016, doi: 10.3390/coatings6030035.
[38] A. Abdelbary and L. Chang, 'Properties and characteristics of tribo-surfaces', in *Principles of Engineering Tribology*, Elsevier, 2023, pp. 33–75. doi: 10.1016/B978-0-323-99115-5.00009-8.
[39] K. Munir, A. Biesiekierski, C. Wen, and Y. Li, 'Surface modifications of metallic biomaterials', in *Metallic Biomaterials Processing and Medical Device Manufacturing*, C. Wen, Ed., Elsevier, 2020, pp. 387–424. doi: 10.1016/B978-0-08-102965-7.00012-6.
[40] E. Thormann, 'Surface forces between rough and topographically structured interfaces', *Curr. Opin. Colloid Interface Sci.*, vol. 27, pp. 18–24, Feb. 2017, doi: 10.1016/j.cocis.2016.09.011.
[41] W. Chrzanowski and F. Dehghani, 'Standardised chemical analysis and testing of biomaterials', in *Standardisation in Cell and Tissue Engineering*, V. Salih, Ed., Elsevier, 2013, pp. 166–197a. doi: 10.1533/9780857098726.2.166.
[42] Q. Xin, 'Friction and lubrication in diesel engine system design', in *Diesel Engine System Design*, Elsevier, 2013, pp. 651–758. doi: 10.1533/9780857090836.3.651.
[43] A. Badarneh, J. J. E. Choi, K. Lyons, J. N. Waddell, and K. C. Li, 'Wear Behaviour of Monolithic Zirconia Against Human Enamel – A Literature Review', *Biotribology*, vol. 32, p. 100224, Sep. 2022, doi: 10.1016/j.biotri.2022.100224.
[44] S. Gowri *et al.*, 'Atomic force microscopy technique for corrosion measurement', in *Electrochemical and Analytical Techniques for Sustainable Corrosion Monitoring*, A. Jeenat, C. Verma, and C. M. Hussain, Eds., Elsevier, 2023, pp. 121–140. doi: 10.1016/B978-0-443-15783-7.00001-3.
[45] Q. Liu, Y. Fu, Z. Qin, Y. Wang, S. Zhang, and M. Ran, 'Progress in the applications of atomic force microscope (AFM) for mineralogical research', *Micron*, vol. 170, p. 103460, Jul. 2023, doi: 10.1016/j.micron.2023.103460.
[46] J. A. Ogilvy, 'A Model for the Ultrasonic Inspection of Rough Defects', in *Non-Destructive Testing*, vol. 1, J. Boogaard and G. M. van Dijk, Eds., Amsterdam: Elsevier, 1989, pp. 830–835. doi: 10.1016/B978-0-444-87450-4.50175-2.
[47] J. Qu, 'Thermomechanical Reliability of Microelectronic Packaging', in *Comprehensive Structural Integrity*, vol. 8, I. Milne, R. Ritchie, and B. Karihaloo, Eds., Elsevier, 2003, pp. 219–239. doi: 10.1016/B0-08-043749-4/08040-X.
[48] F. Quartinello, G. M. Guebitz, and D. Ribitsch, 'Surface functionalization of polyester', in *Methods in Enzymology*, vol. 627, N. Bruns and K. Loos, Eds., Academic Press, 2019, pp. 339–360. doi: 10.1016/bs.mie.2019.08.007.
[49] A. S. Razali, F. L. Supian, S. Abu Bakar, T. H. Richardson, and N. A. Azahari, 'The properties of carbon nanotube on novel calixarene thin film', *Int. J. Nanoelectron. Mater.*, vol. 8, pp. 39–45, 2015.
[50] C. K. D. Lim and F. L. Supian, 'Calix[4]arene and calix[8]arene Langmuir films: Surface studies, optical and structural characterizations', *Int. J. Innov. Technol. Explor. Eng.*, vol. 8, no. 8, 2019.
[51] T. Fujimoto, K. Takeda, and T. Nonaka, 'Airborne Molecular Contamination: Contamination on Substrates and the Environment in Semiconductors and Other Industries', in *Developments in Surface*

Contamination and Cleaning, vol. 1, William Andrew Publishing, 2008, pp. 197–329. doi: 10.1016/B978-0-323-29960-2.00007-1.

[52] J. X. J. Zhang and K. Hoshino, 'Fundamentals of nano/microfabrication and scale effect', in *Molecular Sensors and Nanodevices*, Academic Press, 2018, pp. 43–111. doi: 10.1016/b978-0-12-814862-4.00002-8.

[53] B. S. Yilbas, A. Al-Sharafi, and H. Ali, 'Surfaces for Self-Cleaning', in *Self-Cleaning of Surfaces and Water Droplet Mobility*, Elsevier, 2019, pp. 45–98. doi: 10.1016/b978-0-12-814776-4.00003-3.

[54] A. Mishra, N. Bhatt, and A. K. Bajpai, 'Nanostructured superhydrophobic coatings for solar panel applications', in *Nanomaterials-Based Coatings: Fundamentals and Applications*, Elsevier, 2019, pp. 397–424. doi: 10.1016/B978-0-12-815884-5.00012-0.

[55] A. Boudrioua, M. Chakaroun, and A. Fischer, 'Organic Light-emitting Diodes', in *An introduction to organic lasers*, ISTE Press - Elsevier, 2017, pp. 49–93.

[56] F. L. Supian, D. C. K. Lim, and A. S. Razali, 'Conductivity comparison of calix[8]arene-MWCNTs through spin coating technique', *Sains Malays.*, vol. 46, no. 1, pp. 91–96, Jan. 2017, doi: 10.17576/jsm-2017-4601-12.

[57] A. K. Hassan *et al.*, 'Thin films of calix-4-resorcinarene deposited by spin coating and Langmuir-Blodgett techniques: determination of film parameters by surface plasmon resonance', *Mater. Sci. Eng. C*, vol. 8–9, pp. 251–255, Dec. 1999.

[58] S. Romano *et al.*, 'Optical Biosensors Based on Photonic Crystals Supporting Bound States in the Continuum', *Materials*, vol. 11, no. 4, p. 526, Mar. 2018, doi: 10.3390/ma11040526.

[59] I. Kubicova, J. Skriniarova, D. Pudis, L. Suslik, and M. Vesely, 'Non-Contact NSOM Lithography for 2D Photonic Structure Fabrication', *Phys. Procedia*, vol. 32, pp. 113–116, 2012, doi: 10.1016/j.phpro.2012.03.527.

[60] A. Bakry and S. M. Elmesallamy, 'Sulfonated polypropylene microparticles from waste as adsorbents for methylene blue: Kinetic, equilibrium, and thermodynamic studies', *Sep. Sci. Technol.*, vol. 57, no. 15, pp. 2374–2392, Oct. 2022, doi: 10.1080/01496395.2022.2064874.

[61] N. H. Thang, T. B. Chien, and D. X. Cuong, 'Polymer-Based Hydrogels Applied in Drug Delivery: An Overview', *Gels*, vol. 9, no. 7, p. 523, Jun. 2023, doi: 10.3390/gels9070523.

[62] W. Zhao *et al.*, 'Sulfonate-grafted conjugated microporous polymers for fast removal of cationic dyes from water', *Chem. Eng. J.*, vol. 391, p. 123591, Jul. 2020, doi: 10.1016/j.cej.2019.123591.

[63] Y. Yan, P. Zhou, S.-X. Zhang, X.-G. Guo, and D.-M. Guo, 'Effect of substrate curvature on thickness distribution of polydimethylsiloxane thin film in spin coating process', *Chin. Phys. B*, vol. 27, no. 6, pp. 1–9, Jun. 2018, doi: 10.1088/1674-1056/27/6/068104.

[64] Y. Yan, J. Li, Q. Liu, and P. Zhou, 'Evaporation Effect on Thickness Distribution for Spin-Coated Films on Rectangular and Circular Substrates', *Coatings*, vol. 11, no. 11, pp. 1–16, Oct. 2021, doi: 10.3390/coatings11111322.

[65] K. V. Kumar *et al.*, 'Characterization of the adsorption site energies and heterogeneous surfaces of porous materials', *J. Mater. Chem. A*, vol. 7, no. 17, pp. 10104–10137, 2019, doi: 10.1039/C9TA00287A.

[66] X. Ou, X. Liu, W. Liu, W. Rong, J. Li, and Z. Lin, 'Surface defects enhance the adsorption affinity and selectivity of Mg(OH) $_2$ towards As(<scp>v</scp>) and Cr(<scp>vi</scp>) oxyanions: a combined theoretical and experimental study', *Environ. Sci. Nano*, vol. 5, no. 11, pp. 2570–2578, 2018, doi: 10.1039/C8EN00654G.

[67] M. Takayanagi, N. Fujiwara, R. Seki, M. Sato, and Y. Okuno, 'Amorphous SiO2 Surface Irregularities and their Influence on Liquid Molecule Adsorption by Molecular Dynamics Analysis', *ECS J. Solid State Sci. Technol.*, vol. 12, no. 8, p. 083003, Aug. 2023, doi: 10.1149/2162-8777/acec0e.

[68] I. Isakov *et al.*, 'Quantum Confinement and Thickness-Dependent Electron Transport in Solution-Processed In $_2$ O $_3$ Transistors', *Adv. Electron. Mater.*, vol. 6, no. 11, pp. 1–7, Nov. 2020, doi: 10.1002/aelm.202000682.

[69] F. Güzelçimen *et al.*, 'The effect of thickness on surface structure of rf sputtered TiO2 thin films by XPS, SEM/EDS, AFM and SAM', *Vacuum*, vol. 182, pp. 1–14, Dec. 2020, doi: 10.1016/j.vacuum.2020.109766.

[70] A. Aziz, A. N. Afaah, N. A. M. Asib, R. Mohamed, M. Rusop, and Z. Khusaimi, 'Surface Morphology Studies on Different Layers of PMMA Spin Coated onto Substrate Prepared by Sol-Gel Spin-Coating

Method', *Adv. Mater. Res.*, vol. 1109, pp. 608–612, Jun. 2015, doi: 10.4028/www.scientific.net/AMR.1109.608.

[71] M. A. Basar, S. Debnath, and A. B. Md Ismail, 'An experimental study on the effect of film layer and annealing on morphology by AFM of tin dioxide thin film prepared by spin-coating method', *Mater. Res. Express*, vol. 1, no. 2, p. 026402, May 2014, doi: 10.1088/2053-1591/1/2/026402.

[72] T. Kohoutek *et al.*, 'Surface morphology of spin-coated As–S–Se chalcogenide thin films', *J. Non-Cryst. Solids*, vol. 353, no. 13–15, pp. 1437–1440, May 2007, doi: 10.1016/j.jnoncrysol.2006.10.068.

[73] A. R. Arul, H. B. Ramalingam, R. Balamurugan, and R. Venckatesh, 'Optically rough TiO2 thin film surface study by laser speckle photography', in *Materials Today: Proceedings*, 2023, pp. 1381–1384. doi: 10.1016/j.matpr.2023.05.535.

[74] A. Beena Unni, R. Winkler, D. M. Duarte, K. Chat, and K. Adrjanowicz, 'Influence of Surface Roughness on the Dynamics and Crystallization of Vapor-Deposited Thin Films', *J. Phys. Chem. B*, vol. 126, no. 40, pp. 8072–8079, Oct. 2022, doi: 10.1021/acs.jpcb.2c04541.

[75] K. Kalantari, B. Saleh, and T. J. Webster, 'Applications of Thin Films in Metallic Implants', in *Materials for Devices*, Boca Raton: CRC Press, 2022, pp. 271–304. doi: 10.1201/9781003141358-10.

[76] M. Mozetič, 'Surface Modification to Improve Properties of Materials', *Materials*, vol. 12, no. 3, p. 441, Jan. 2019, doi: 10.3390/ma12030441.